

# Unraveling the function of the two Entner–Doudoroff branches in the thermoacidophilic Crenarchaeon *Sulfolobus solfataricus* P2

Theresa Kouril<sup>1</sup>, Patricia Wieloch<sup>2</sup>, Julia Reimann<sup>3</sup>, Michaela Wagner<sup>3</sup>, Melanie Zaparty<sup>4</sup>, Sonja-Verena Albers<sup>3</sup>, Dietmar Schomburg<sup>2</sup>, Peter Ruoff<sup>5</sup> and Bettina Siebers<sup>1</sup>

<sup>1</sup> Molecular Enzyme Technology and Biochemistry, Biofilm Centre, Faculty of Chemistry, University of Duisburg-Essen, Germany

<sup>2</sup> Department of Bioinformatics and Biochemistry, Technische Universität Braunschweig, Germany

<sup>3</sup> Molecular Biology of Archaea, Max-Planck-Institute for Terrestrial Microbiology, Marburg, Germany

<sup>4</sup> Institute for Molecular and Cellular Anatomy, University of Regensburg, Germany

<sup>5</sup> Faculty of Science and Technology, Centre of Organelle Research, University of Stavanger, Norway

## Keywords

carbohydrate metabolism; Entner–Doudoroff pathway; glycerate kinase; metabolomics; thermophiles

## Correspondence

B. Siebers, Molecular Enzyme Technology and Biochemistry, Biofilm Centre, Faculty of Chemistry, University of Duisburg-Essen, Universitätsstrasse 5, 45141 Essen, Germany

Fax: +49 201 183 6603

Tel: +49 201 183 7061

E-mail: [bettina.siebers@uni-due.de](mailto:bettina.siebers@uni-due.de)

(Received 13 July 2012, revised 17 December 2012, accepted 19 December 2012)

doi:10.1111/febs.12106

*Sulfolobus solfataricus* P2 is a thermoacidophilic archaeon that metabolizes glucose and galactose via an unusual branched Entner–Doudoroff (ED) pathway, which is characterized by a non-phosphorylative (np) and a semi-phosphorylative (sp) branch. However, so far the physiological significance of the two pathway branches is unknown. In order to address these questions two key enzymes of the branched ED pathway, the class II glycerate kinase (GK) of the np-ED branch and the 2-keto-3-deoxygluconate kinase (KDGK) of the sp-ED branch in *S. solfataricus*, were investigated. GK was recombinantly purified and characterized with respect to its kinetic properties. Mg<sup>2+</sup> dependent Sso-GK (glycerate + ATP → 2-phosphoglycerate + ADP) showed unusual regulatory properties, i.e. substrate inhibition and cooperativity by D-glycerate and ATP, and a substrate-inhibition model was established fitting closely to the experimental data. Furthermore, deletion of the sp-ED key enzyme KDGK in *S. solfataricus* PBL2025 resulted in a similar growth phenotype on glucose as substrate compared with the wild-type. In contrast, the mutant showed strongly increased concentrations of np-ED intermediates whereas the hexose and pentose phosphates as well as trehalose were decreased. Together the results indicate (a) that the np-ED pathway is able to compensate for the missing sp-ED branch in glucose catabolism, (b) that in addition to its catabolic function the sp-ED pathway has an additional although not essential role in providing sugar phosphates for anabolism/gluconeogenesis and (c) that GK, with its unusual regulatory properties, seems to play a major role in controlling the flux between the glycolytic np-ED and the glycolytic/gluconeogenetic sp-ED pathway.

## Database

The amino acid sequence data of GK of *S. solfataricus* P2 is available in the UniProt Protein Database under the accession number [Q7LXP1](http://www.uniprot.org/uniprot/Q7LXP1) (<http://www.uniprot.org/uniprot/Q7LXP1>).

## Abbreviations

2PG, 2-phosphoglycerate; 3PG, 3-phosphoglycerate; ED, Entner–Doudoroff; EMP, Embden–Meyerhoff–Parnas; F6P, fructose 6-phosphate; G6P, glucose 6-phosphate; GAP, glyceraldehyde 3-phosphate; GAPN, non-phosphorylating GAP dehydrogenase; GK, glycerate kinase; KD(P)GA, KD(P)G aldolase; KDG, 2-keto-3-deoxygluconate; KDGK, 2-keto-3-deoxygluconate kinase; KDPG, 2-keto-3-deoxy-6-phosphogluconate; MOFRL, multi-organism fragment with rich leucine; np, non-phosphorylative; sp, semi-phosphorylative; Xyl5P, xylulose 5-phosphate.

## Introduction

The coexistence of three domains of life with two prokaryotic lineages, Bacteria and Archaea, beside Eukaryotes was established about 30 years ago [1]. Like Bacteria and simple Eukaryotes, Archaea exhibit a complex central carbohydrate metabolism, utilizing glucose via modifications of the classical Embden–Meyerhof–Parnas (EMP) and the Entner–Doudoroff (ED) pathway [2–4]. The thermoacidophilic aerobic Crenarchaeon *Sulfolobus solfataricus* P2 grows optimally at 80 °C and pH 2–4 (strain P2) [5]. Glucose catabolism in *S. solfataricus* proceeds via an unusual branched ED pathway comprising a non-phosphorylative (np) and a semi-phosphorylative (sp) branch, which is promiscuous and represents an equivalent route for glucose and galactose catabolism [6–8]. Conversely, the EMP pathway in this organism is supposed to function exclusively in gluconeogenesis due to the lack of a functional phosphofructokinase (Fig. 1).

In the common part of the branched ED pathway, glucose is first oxidized to gluconate by glucose dehydrogenase [7,9], which is further dehydrated via gluconate dehydratase [10,11] to 2-keto-3-deoxygluconate (KDG). In the sp-ED branch KDG is then phosphorylated by KDG kinase (KDGK) [12] to 2-keto-3-deoxy-6-phosphogluconate (KDPG) which is further cleaved by KD(P)G aldolase (KD(P)GA) [8,10,12] into one molecule of glyceraldehyde 3-phosphate (GAP) and pyruvate. Further degradation of GAP is catalyzed by an NADP<sup>+</sup> dependent non-phosphorylating GAP dehydrogenase (GAPN) [13] yielding 3-phosphoglycerate (3PG) and NAD(P)H + H<sup>+</sup>. Via phosphoglycerate mutase [14], enolase and pyruvate kinase 3PG is metabolized in the common lower EMP shunt yielding a second molecule of pyruvate. In contrast, in the np-ED branch, KDG is not phosphorylated but is directly cleaved by the same bifunctional KD(P)GA into pyruvate and glyceraldehyde, and glyceraldehyde is oxidized to glycerate and reduced ferredoxin by ferredoxin-dependent aldehyde oxidoreductase [15] (in contrast to the NAD(P)<sup>+</sup> dependent GAP oxidation in the sp-ED branch). Then glycerate kinase (GK) converts glycerate to 2-phosphoglycerate (2PG), which is further degraded via the common lower shunt of the EMP pathway. Thus, in both pathway branches no net energy is produced in the form of ATP and the major source of energy appears to be the aerobic respiratory chain. Although the enzymology of the branched ED pathway in *S. solfataricus* is meanwhile quite well understood the physiological significance and the regulation of the sp-ED and the np-ED branches and the flux distribution between both

pathway branches remain unclear. The utilization of the np- instead of the sp-ED branch avoids the formation of the extremely heat-labile GAP, dihydroxyacetonephosphate as well as 1,3-bisphosphoglycerate [8,13] and it has been suggested previously that the presence of the two branches might have an important role in thermoadaptation of organisms growing at high temperatures [8].

KDGK and GK represent key enzymes of the sp-ED and the np-ED branches, respectively. GKs are found in all three domains of life and are grouped into three main classes (class I, II, III) which share no common origin [16,17]. According to databank searches, archaeal GKs, including the GK from *S. solfataricus*, represent members of class II [GK II, MOFRL (multi-organism fragment with rich leucine) family [16]], catalyzing the phosphoryltransfer from ATP to the substrate glycerate yielding 2PG. Archaeal GKs from *Thermoplasma acidophilum* [18], *Picrophilus torridus* [17], *Pyrococcus horikoshii* [19], *Sulfolobus tokodaii* [20] and *Thermoproteus tenax* [16] have been characterized. All these archaeal GKs differ in (co)substrate specificity and affinity as well as their specificity towards metal ion required for optimal activity. In Bacteria a central role of GK in other metabolic pathways like the serine cycle, glycolate metabolism and tartrate utilization has been established [16,19,21].

KDGK genes have been identified in the *T. tenax* and also in the *S. solfataricus* genome as part of the ED gene cluster together with the genes encoding the gluconate dehydratase (*gad*), the KD(P)GA (*kdgA*) and the GAPN (*gapN*) (*S. solfataricus*) or a glycoamylase (*T. tenax*), respectively. The coding function was proved by recombinant expression, partial purification and enzyme measurements [8]. The Sso-KDGK has been purified to homogeneity, the kinetic parameters have been determined and it could be demonstrated that also the KDGK in *S. solfataricus* is promiscuous using KDG and 2-keto-3-deoxy-D-galactonate as substrates [12]. Also, the crystal structure of the enzyme from *S. solfataricus* has been reported suggesting that the spatial reorientation of residues compared with non-promiscuous KDGK might be responsible for the substrate promiscuity of the enzyme [22].

In order to unravel the physiological function of the two ED branches the enzymatic and regulatory properties of the GK of *S. solfataricus* were determined. The GK encoding gene (SSO0666, *garK*) was cloned and expressed in *Escherichia coli* BL21(DE3)-RIL and the recombinant protein was purified and biochemically characterized. Furthermore, a KDGK deletion

mutant was constructed, which specifically shuts down the sp-ED branch. The effect of the deletion was analyzed by growth studies and by comparative metabolic fingerprinting.

## Results

### Enzyme characterization of Sso-GK

#### Cloning, expression and purification of the recombinant GK

The gene homolog of the archaeal class II glycerate kinase (SSO0666) from *S. solfataricus* was cloned into the pET vector system using PCR mutagenesis. GK (EC 2.7.1.165) was purified to homogeneity using three different purification steps (heat precipitation, anion exchange chromatography and gel filtration; Fig. 2). Two milligrams of pure protein was obtained from 12 g (wet weight) of *E. coli* cells with a maximum specific activity of 35 U·mg<sup>-1</sup> at 80 °C after gel filtration. The subunit size of GK was 49 kDa as derived from SDS/PAGE, which corresponds well to the theoretically calculated mass of 44.4 kDa (Fig. 2). A native molecular mass of ~90 kDa was determined by gel filtration indicating a homodimeric structure of the GK.

#### Kinetic parameters

Sso-GK catalyzed the ATP-dependent phosphorylation of glycerate to 2PG and ADP. The formation of 3PG was not detected. The enzyme was specific for D-glycerate; the use of a mixture of D- and L-glycerate resulted in only ~40% activity, which is in accordance with previous observations [16]. Rate dependences on D-glycerate and ATP concentrations were determined at 80 °C, the optimal growth temperature of the organism (Fig. 3). For D-glycerate, substrate inhibition was observed at glycerate concentrations higher than 2 mM (Fig. 3).

Data analysis was performed up to the determined maximal specific activity, omitting the inhibitory substrate concentrations using the Hill equation in order to describe the cooperative behavior of GK. The kinetic parameters obtained were  $V_{\max} = 38 \text{ U}\cdot\text{mg}^{-1}$ ,  $K_s = 1 \text{ mM}$  and a Hill constant of  $2.6 (\pm 0.9)$  (Table 1). However, the kinetic data derived by curve fitting using the Hill equation have only indicative value, since curve fitting was only performed for the monotonic increasing part of the specific activity, where no obvious inhibition is observed.

In addition to the parameter estimation using the Hill equation, data analyses were performed using the

established model in Fig. 4. The results were in good agreement with the experimentally observed data over the whole substrate concentration range of glycerate including the inhibitory concentrations ( $R = 0.99266$ ). In the model, a cooperativity of 2 (in agreement with Hill) was implemented, i.e. two molecules of substrate bind to the enzyme, where the active complex leading to product was written as  $ES_2$  (Fig. 4). Fitting with the kinetic model resulted in the following kinetic data:  $V_{\max} = 851 \text{ U}\cdot\text{mg}^{-1}$ ,  $K_i = 0.1 \text{ mM}$ ,  $K_s = 48 \text{ mM}$  (Table 1). The good fit achieved from the model (Fig. 4) to the experimental data suggested a mechanism where two glycerate molecules bind to GK and are converted to product, while a third binding site appears to be inhibitory. The model suggested that the inhibition appears to be due to the formation of an additional complex ( $ES_3$ ) with very low activity at 80 °C [~1% of the product (per min) was formed by the inhibitory complex  $ES_3$ ] indicated by the  $\alpha$ -value ( $\alpha = 0.01$ ). The  $K_i$  value of 0.1 mM for glycerate indicated a stable inhibitory complex  $ES_3$ . Rate dependences on D-glycerate were also determined at 70 and 65 °C and substrate inhibition was observed as well at glycerate concentrations above 2 mM at 70 °C and 5 mM at 65 °C (Fig. 3A).

Kinetic analysis on the cofactor ATP in the presence of 2 mM glycerate was performed. ATP-dependent analysis showed weak substrate inhibition and kinetic parameters were determined using two kinetic models (Fig. 3B); whereas fit I reflects standard Michaelis–Menten kinetics, fit II was performed using the non-cooperative Michaelis–Menten substrate-inhibition model (see Fig. S1 for mechanism). The  $V_{\max}$  values for ATP were in the same range as those for D-glycerate (Hill equation), i.e.  $V_{\max}$  values of  $46 \text{ U}\cdot\text{mg}^{-1}$  or  $56 \text{ U}\cdot\text{mg}^{-1}$  with  $K_s$  values for ATP of  $0.9 (\pm 0.2) \text{ mM}$  and 1.5 mM for fit I or fit II, respectively (Table 1). The inhibition by ATP turned out to be very low, as reflected by a  $K_i$  value of 61 mM.

### Analysis of KDGK deletion strain of *S. solfataricus*

#### Deletion of the 2-keto-3-deoxygluconate kinase gene in *S. solfataricus*

In addition to the GK characterization, the physiological role and the pathway selection of both the sp-ED and the np-ED branches *in vivo* in *S. solfataricus* was further studied by disrupting the 2-keto-3-deoxygluconate kinase (*kdgK*) gene in *S. solfataricus* PBL2025 (Fig. S2). For (in-frame) gene deletion in PBL2025 the established genetic system was used [23–25]. The locus



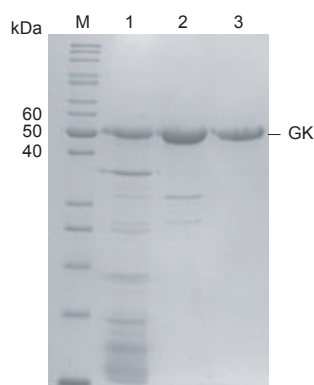


**Fig. 2.** Purification of the recombinant GK of *S. solfataricus*. Coomassie stained SDS/PAGE of GK fractions after different purification steps: 1, supernatant after heat precipitation (20 min, 80 °C); 2, GK fraction after anion exchange chromatography; 3, purified enzyme after gel filtration; M, marker. PageRuler™ Unstained Protein Ladder (Fermentas).

they show no high sequence similarity to the characterized KDGK (SSO3195; relevant hits SSO0004, *e*-value  $4e-09$ ; SSO2449, *e*-value  $6e-06$ ). Therefore, assuming the absence of other KDG phosphorylating enzymes the deletion leads to a specific shutdown of the sp-ED branch. The *kdgk* gene is the last gene of an operon comprising *gad* and *kdgA*. The *gapN* gene is localized around 80 bp downstream. For both the *gad-kdgA-kdgk* operon and the *gapN* gene the respective transcription start sites have been mapped [13]. In order to exclude that the *kdgK* deletion affects transcription of the co-organized genes qRT-PCR studies for *gapN*

(SSO3194) and *kdgA* (SSO3197) were performed in the mutant in comparison with the wild-type strain. The study revealed a slight increase in RNA levels for *kdgA* (3.8-fold) and *gapN* (2.2-fold) in the *kdgk* deletion strain (Fig. S3). However, both genes are still transcribed confirming that the observed growth effects are due to the *kdgk* deletion and not to dramatic changes (i.e. downregulation) of adjacent genes.

### Growth phenotype of the KDGK deletion strain (PBL2025Δ3195) under glycolytic conditions

The KDGK deletion strain (PBL2025Δ3195) was analyzed in comparison with the reference strain PBL2025 regarding growth on glucose in Brock minimal medium at 76 °C. The PBL2025Δ3195 deletion strain showed growth properties on glucose that are not distinguishable from those of the host strain PBL2025 with a doubling time of 12 h (Fig. 5).

### Comparative metabolome analyses of PBL2025Δ3195 and PBL2025

In order to analyze the effect of the KDGK deletion in more detail metabolome analyses were performed following the established protocol for *S. solfataricus* using GC-MS [26]. A comparison between determined metabolites in *S. solfataricus* PBL2025 and PBLΔ3195 identified 282 peaks. Of these, 75 could be matched to known compounds belonging to primary metabolism by comparison with available mass spectral libraries. Thirteen compounds represented unknown

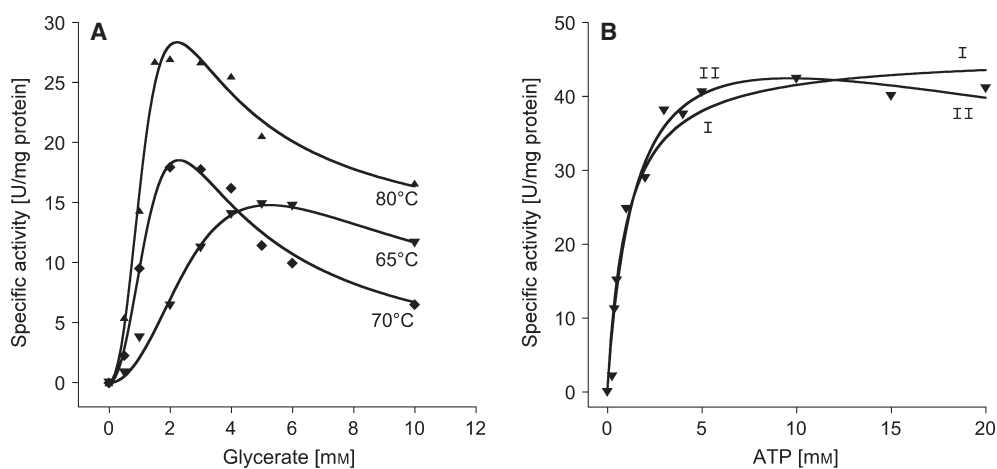


**Fig. 3.** Sso-GK activity. Nonlinear curve fit to the experimental data points for D-glycerate at 80, 70 and 65 °C (A) and ATP at 80 °C (B). For glycerate the kinetic model (Fig. 4) was used. For ATP curve I shows the fit using standard Michaelis–Menten kinetics, while curve II shows the fit using the non-cooperative model with ATP substrate inhibition. Curve fits were performed using KALEIDAGRAPH. For parameter values see Table 1.



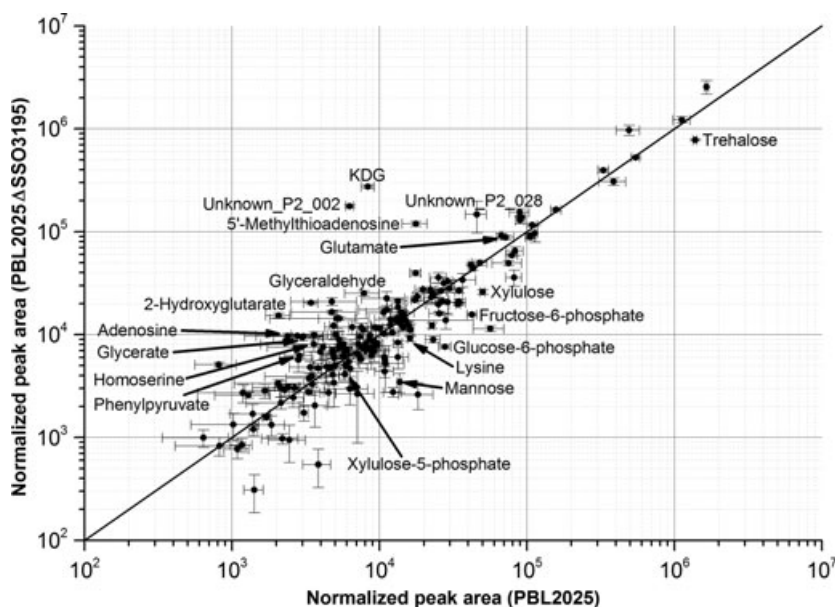


**Fig. 6.** Plot of logarithmically transformed metabolite concentrations from *S. solfataricus* strains PBL2025 and PBL2025Δ3195.

**Table 2.** Changes in metabolite levels of the central carbohydrate metabolism of PBL2025Δ3195 in comparison with PBL2025.

Metabolites	Ratio
ED pathway (glycolysis)	
KDG	32.7, up
Glyceraldehyde	3.2, up
Glycerate	3.1, up
EMP pathway (gluconeogenesis)	
Fructose 6-phosphate	0.4, down
Glucose 6-phosphate	0.3, down
Trehalose metabolism (compatible solute)	
Trehalose	0.5, down
RuMP pathway (pentose metabolism)	
Xylulose 5-phosphate	0.7, down

molecular mass of 90 kDa was observed indicating a homodimeric structure of Sso-GK (subunit 49 kDa). This suggests that each subunit harbors one active center with the binding sites for each, ATP and glycerate. Also, most of the GKs of the MORFL family described so far represent homodimers [17,19,20] or monomers [16,18]. For the crystallized enzyme from *T. maritima* gel filtration and light scattering revealed a homodimeric structure whereas in crystals the enzyme appeared to be monomeric.

Sso-GK showed a complex regulation including cooperativity and substrate inhibition for glycerate. For ATP, kinetics of standard Michaelis–Menten type were observed as well as slight ATP inhibition. Although the observed positive cooperativity ( $n = 2.6$ ) for the Sso-GK fits quite well with the homodimeric structure

harboring two active sites positively influencing substrate affinity of one another, cooperativity has not been described for any of the GKs characterized so far. However, substrate inhibition was previously shown for the GK from the hyperthermophilic Crenarchaeon *T. tenax* [16], whereas for GKs from other (hyper)thermophilic organisms such as *P. torridus*, *P. horikoshii* or *T. maritima* [17,19,21] no inhibition has been reported (Table 3). Substrate inhibition was also not reported for the recently characterized GK from *S. tokodaii* [20], although the proteins exhibit 52% amino acid sequence identity. However, the specific activities of the characterized GKs are 10- to 100-fold higher than the maximal specific activity observed for the inhibited enzymes (*T. tenax*, *S. solfataricus*; Table 3). From the established kinetic model, which considers the inhibitory substrate concentrations, 10-fold higher  $V_{\max}$  values were calculated for the *S. solfataricus* GK which are in the same range as described for the not substrate inhibited GKs characterized so far. This finding indicates that the  $K_i$  value is the determining rate parameter of Sso-GK. Thus, with its cooperative behavior as well as the substrate inhibition, Sso-GK could be a major control point in the np-ED branch directly responding to the glycerate concentrations in the cell. Sso-GK activity will be enhanced with lower glycerate concentrations and decreased at high concentrations and thereby reducing the flux through the np-ED branch.

In addition to the characterization of the np-ED key enzyme GK, a deletion mutant of the *kdgk* gene was

established (PBL2025Δ3195) which specifically shuts down the sp-ED branch. The phenotype was analyzed by growth studies on glucose as well as by metabolome analyses. The KDGK deletion strain revealed no difference in glycolytic growth compared with the reference strain PBL2025. Therefore under the applied growth conditions *S. solfataricus* does not rely on an active sp-ED pathway indicating that the np-ED branch or other pathways can easily substitute for the sp-ED branch.

However, metabolomic analyses revealed a significant upregulation of intermediates of the np-ED branch in the deletion mutant (KDG 33-fold, glyceraldehyde three-fold, glycerate three-fold; Table 2). The dramatic increase of KDG and other np-ED metabolites supports the homology based prediction that SSO3195 is the only KDGK in *S. solfataricus* P2 and confirms the complete shutdown of the sp-ED branch by deletion of the encoding gene. Furthermore, it indicates that in the wild-type there is appreciable flux through the sp-ED branch during glycolysis, which is rerouted in the KDGK deletion strain. For the characterized KD(P)GA of *S. solfataricus* a strong preference for the phosphorylated substrate KDPG with a catalytic efficiency ( $k_{\text{cat}}/K_{\text{m}}$  value) of  $643 \text{ mM}^{-1}\cdot\text{s}^{-1}$  compared with  $1.1 \text{ mM}^{-1}\cdot\text{s}^{-1}$  for KDG was reported [12]. This significantly reduced activity towards KDG in combination with the substrate inhibition of GK by elevated glycerate concentrations presumably leads to the accumulation of np-ED metabolites. Substrate inhibition of Sso-GK might also limit the *in vivo* flux into the lower shunt of the np-ED branch in the wild-type strain. However, under wild-type conditions np-ED intermediate accumulation is prevented by the action of the sp-ED branch in combination with anabolic purposes (see below). Thus, GK appears to function as a throttle valve in the np-ED branch thereby regulating the flux via both ED branches into the lower common shunt of the EMP pathway (Fig. 1). Such sophisticated glycolytic flux control might be useful, as the flux

directly enters the citric acid cycle and therefore influences the flux of several connected metabolic and biosynthetic pathways, e.g. amino acid metabolism.

Interestingly, the KDGK deletion also had an obvious effect on hexose phosphates, pentose phosphates and trehalose (G6P, F6P, Xyl5P and trehalose decreased by factors between 2 and 4) suggesting that the sp-ED has an additional important gluconeogenetic function (Table 2, Fig. 1). Hence, GAP produced from KDG via KDGK and KD(P)GA seems to be partially utilized for gluconeogenesis (i.e. GAP is converted to F6P via reverse EMP); thus the decrease in F6P, G6P and Xyl5P might be due to the missing supply of GAP. This finding suggests that the np-ED is purely catabolic, whereas sp-ED displays both catabolic and anabolic features. However, since no obvious phenotype was observed upon glycolytic growth other pathways seem to contribute or substitute in order to sufficiently provide hexose phosphates as building blocks for pentoses, glycogen and trehalose in anabolism. Hexose phosphate formation starting from 2PG via the reversed EMP pathway (after glucose has been processed by the np-ED branch) seems to be energetically less favorable, because it requires additional ATP at the level of 3PG phosphorylation via phosphoglycerate kinase. Thus, bypassing phosphoglycerate kinase/GAP dehydrogenase reactions in anabolism by means of KDGK and KD(P)GA in the sp-ED branch is energetically more efficient. In addition to the reported glucose degradation via the branched ED pathway in *S. solfataricus* P2 also ATP-dependent hexokinase activity was detected in cell-free extracts ( $0.0025 \text{ U}\cdot\text{mg}^{-1}$ ,  $80 \text{ }^{\circ}\text{C}$ ) although a functional catabolic EMP pathway is missing. Hexokinase activity has been previously reported in crude extracts of *Sulfolobus* strain MT4 ( $0.008 \text{ U}\cdot\text{mg}^{-1}$ ,  $70 \text{ }^{\circ}\text{C}$ ) [6]. Furthermore, the hexokinase from *S. tokodaii* which exhibits broad substrate specificity has been characterized previously (ST2354) and the crystal structure has been solved [27,28]. Therefore, next to the sp-ED

**Table 3.** Comparison of kinetic parameters of class II GK for D-glycerate from (hyper)thermophilic organisms. A, Archaea; B, Bacteria; n.d., not determined.

Organism	Assay $T$ ( $^{\circ}\text{C}$ )	$V_{\text{max}}$ ( $\text{U}\cdot\text{mg}^{-1}$ )	$K_{\text{S}}$ (mM)	Amino acid identity (%)	Reference
<i>Sulfolobus solfataricus</i> (A)	80	851 (33) <sup>a</sup>	48 (1.0) <sup>a</sup>	100	This study
<i>Sulfolobus tokodaii</i> (A)	80	1302 <sup>b</sup>	n.d.	52	20
<i>Pyrococcus horikoshii</i> (A)	45	624.46	0.044	37	19
<i>Picrophilus torridus</i> (A)	50	435	0.34	35	17
<i>Thermotoga maritima</i> (B)	37	n.d.	0.15	33	21
<i>Thermoproteus tenax</i> (A)	70	15.05 <sup>c</sup>	0.02	31	16
<i>Thermoplasma acidophilum</i> (A)	50	118 <sup>d</sup>	0.56	30	18

<sup>a</sup> Parameters derived from the kinetic model and the Hill equation. <sup>b</sup> Reported specific activity. <sup>c</sup> Since glycerate inhibition is observed for the *T. tenax* enzyme the estimated values for up to 0.3 mM glycerate are given. <sup>d</sup> Determined for D,L-glycerate.

branch, hexokinase might be used as an alternative way to generate hexose phosphates and thus pentoses, trehalose and glycogen directly from glucose (Fig. 1). The synthesis of hexose phosphates as precursors via hexokinase requires no additional ATP compared with the sp-ED pathway where ATP is required for KDG phosphorylation via KDGK and therefore might represent an efficient alternative route. As presented here, except for the change in concentration of np-ED intermediates and some sugar phosphates, the elimination of the sp-ED branch has no serious effects on growth and the general stability of the metabolism as judged from the metabolome analysis is quite remarkable. Therefore previous concepts [29] that the np-ED branch might play an important role in metabolic thermoadaptation by omitting the thermolabile intermediates GAP, dihydroxyacetonephosphate and 1,3-bisphosphoglycerate and thus allowing for energy optimization can be ruled out at least for growth at optimal conditions, such as 76 °C. In accordance with this concept the absence of the sp-ED branch in the KDGK deletion strain should result in a significantly improved growth on glucose, which is not observed. However, for final evaluation future studies at temperatures below or above the growth optimum as well as analysis of the generation of hexose phosphates are awaited, which might require additional energy investment. In summary this study highlights the metabolic flexibility and robustness of *S. solfataricus* harboring alternative routes, i.e. via hexokinase, to provide precursors for metabolic pathways linked to the branched ED pathway. In addition the kinetic properties of GK with strong inhibition by glycerate seem to allow regulating the flux, as throttle valve, between the glycolytic np-ED and glycolytic/gluconeogenic sp-ED pathway in response to the cellular glycerate concentration.

## Experimental procedures

### Cloning, expression and purification of recombinant GK

The *garK* gene (SSO0666) was amplified by PCR mutagenesis using the following primer set (restriction sites underlined): *garK* forward primer, 5'-GGGGAATTCCA TGGATATTGTTGATAAGATATTAG-3'; *garK* reverse primer, 5'-GGGGGATCCTCAAGGAGCCCTTAAGAC-3'.

After digestion (*Nco*I and *Bam*HI) and ligation, the constructed vector *garK*-pET324 [31] was introduced into *E. coli* BL21(DE3)-RIL (Agilent Technologies, Ratingen, NRW, Germany). Cells were grown at 37 °C and 180 r.p.m. in LB medium (pH 7; LB broth; Sigma-Aldrich, Tauf-

kirchen, Germany) supplemented with 100 µg·mL<sup>-1</sup> ampicillin and 34 µg·mL<sup>-1</sup> chloramphenicol. At an optical density of 0.6–0.8 expression of GK was induced by adding 1 mM isopropyl β-D-1-thiogalactopyranoside. After 3 h, cells were harvested by centrifugation (20 min, 6000 g, 4 °C) and suspended in 100 mM HEPES/KOH (pH 7.0) containing 5 mM dithiothreitol, 1 g cells (wet weight) in 3 mL buffer. Cell-free extract was obtained by ultrasonic disruption followed by centrifugation (45 min, 16 000 g, 4 °C). The supernatant was diluted 1 : 1 with resuspension buffer and heat precipitation was performed (80 °C for 20 min). After centrifugation (30 min at 16 000 g, 4 °C) the clear supernatant was dialyzed against 20 mM HEPES/KOH, 5 mM dithiothreitol (pH 9.0, room temperature) and applied to an anion exchange column (UNO Q-12 column; Bio-Rad Laboratories, München, Germany) pre-equilibrated with the same buffer. All GK activity was found in the flow-through fraction and was subsequently separated via gel filtration (HiLoad 26/60 Superdex200 prep grad column; Amersham Biosciences, Glattbrugg, Switzerland) using 50 mM HEPES/KOH (pH 7, room temperature), 300 mM KCl and 5 mM dithiothreitol as the mobile phase. Fractions containing GK were collected and dialyzed overnight against 100 mM HEPES/KOH, 5 mM dithiothreitol (pH 7.0).

### Enzyme assays

The enzymatic activity was determined in a discontinuous assay by coupling product formation (ADP or 2PG, respectively) at high temperature (65, 70 and 80 °C) to the oxidation of NADH via mesophilic auxiliary enzymes.

The standard assay mixture (800 µL total volume) contained 100 mM HEPES (pH 6.5 at the respective temperature), 20 mM MgCl<sub>2</sub>, 5 mM ATP, 1 mM glycerate, 5 mM EGTA and 1 µg purified GK. EGTA was included in the assay because Ca<sup>2+</sup>, which is present in commercial preparations of D-glycerate (D-(+)-glyceric acid hemicalcium salt hydrate), was found to inhibit *S. solfataricus* GK as well as GKs in general [18]. The assay mixture was pre-incubated at the indicated temperatures and the reaction was started by the addition of D-glycerate. At times of 0, 0.5, 1, 1.5, 2 and 2.5 min aliquots were withdrawn and the reaction was stopped by incubation on ice.

### ADP formation

The amount of ADP formed was quantified using mesophilic auxiliary enzymes in HEPES/KOH (pH 7) buffer containing 20 mM MgCl<sub>2</sub>, 0.5 mM NADH, 2 mM phosphoenolpyruvate, 4 U lactate dehydrogenase (rabbit muscle, [EC 1.1.1.27](#); Sigma-Aldrich) and 8 U pyruvate kinase (rabbit muscle, [EC 2.7.1.40](#); Sigma-Aldrich) (500 µL total volume). The oxidation of NADH to NAD<sup>+</sup> was followed in a Spectord 210

Photometer at 340 nm (Analytik Jena,  $\epsilon_{\text{NADH}} = 6.3 \text{ mM}^{-1}\cdot\text{cm}^{-1}$ ). This assay was used for the determination of kinetic parameters in the presence of 0–10 mM ATP or D-glycerate and fixed concentrations of 2 mM D-glycerate (5 mM at 65 °C) or 5 mM ATP, respectively.

## 2PG or 3PG formation

In order to confirm 2PG formation instead of 3PG two other indicator assays were used (100 mM HEPES/KOH, pH 7, 500  $\mu\text{L}$  total volume, 37 °C): (a) the assay system for 2PG detection contained 2 U enolase (*Saccharomyces cerevisiae*, EC 4.2.1.11; Sigma-Aldrich), 10 mM ADP, 20 mM  $\text{MgCl}_2$ , 0.5 mM NADH, 8 U pyruvate kinase and 4 U lactate dehydrogenase; (b) the assay for 3PG detection contained 10 U 3-phosphoglycerate kinase (*S. cerevisiae*, EC 2.7.2.3; Sigma-Aldrich), 10 U glyceraldehyde 3-phosphate dehydrogenase (rabbit muscle, EC 1.2.1.12; Sigma-Aldrich), 5 mM ATP, 10 mM  $\text{MgCl}_2$  and 0.5 mM NADH in 100 mM HEPES/KOH (pH 7, room temperature). Control reactions were performed without substrate and enzyme, respectively, for all listed assays.

## Kinetic models

### Glycerate kinetics

A model (based on the experimental data) for the conversion of D-glycerate by GK at constant ATP concentration was developed (Fig. 6). The basic feature of the model includes two substrate binding sites with positive cooperativity leading irreversibly to the product of two molecules of 2PG. Increased amounts of substrate inhibit the activity of the enzyme by the addition of another substrate molecule leading to a much less reactive enzyme–substrate complex  $\text{ES}_3$ . As will be shown below, the model suggests that  $\text{ES}_3$  has some residual activity at 80 °C but practically none at lower temperatures.

Considering the reactions in Fig. 6 as elementary processes, the following rate equation can be formulated (for the derivation, see Doc. S1):

$$v = \frac{V_{\max}[\text{S}]^2}{K_S + [\text{S}]^2 + [\text{S}]^3/K_i} \left(1 + \alpha \frac{[\text{S}]}{K_i}\right) \quad (1)$$

where  $\alpha = 3k_2/2k_{\text{cat}}$ ,  $V_{\max} = 2k_{\text{cat}}[\text{E}]_{\text{tot}}$  with  $[\text{E}]_{\text{tot}}$  the total enzyme and  $K_S$  is the substrate concentration at which the reaction rate is half the  $V_{\max}$  concentration. Equation (1) was fitted to experimental data at different temperatures using the program KALEIDAGRAPH (www.synergy.com).

### Hill equation

The cooperativity of ATP and glycerate kinetic data was analyzed by the Hill equation (Eqn 2) by varying  $K_S$ , the maximum velocity  $V_{\max}$  and the cooperativity  $n$  using the software

KALEIDAGRAPH (Synergy Software, Reading, PA, USA) and ORIGIN (OriginLab Corporation, Northampton, MA, USA).

$$v = \frac{V_{\max}[\text{S}]^n}{(K_S)^n + [\text{S}]^n} \quad (2)$$

where S is either ATP or D-glycerate.

## ATP kinetics

ATP kinetic data at constant glycerate concentration were also fitted to Eqn (3) when ATP shows substrate inhibition under non-cooperative conditions. The mechanism is shown in Fig. S1.

$$v = \frac{V_{\max}[\text{ATP}]}{K_S + [\text{ATP}] + [\text{ATP}]^2/K_i} \quad (3)$$

In addition, standard Michaelis–Menten kinetics (Eqn 4) were also used:

$$v = \frac{V_{\max}[\text{ATP}]}{K_M + [\text{ATP}]} \quad (4)$$

## Cultivation of *S. solfataricus* strain P2 (DSM 1617), preparation of crude extract and hexokinase assay

*S. solfataricus* P2 cultures were cultivated on glucose under standardized growth conditions and crude extracts were prepared following an established standard protocol as described previously [26]. Hexokinase activity was determined in a discontinuous assay at 80 °C by incubating 2 mg crude extract, 20 mM glucose, 10 mM ATP, 20 mM  $\text{MgCl}_2$  and 100 mM HEPES/KOH buffer (pH 6.5, 80 °C) in a total volume of 400  $\mu\text{L}$ . Aliquots (100  $\mu\text{L}$ ) were withdrawn after 0, 4, 8 and 12 min and stored on ice. The amount of G6P produced was determined at 25 °C by using 5 U G6P dehydrogenase (*S. cerevisiae*; Sigma-Aldrich) in an assay mixture of 500  $\mu\text{L}$  comprising 100 mM HEPES/KOH (pH 7, room temperature) and 5 mM  $\text{NADP}^+$ .

## Disruption of the *kdgK* gene in *S. solfataricus* PBL2025 and growth conditions

The *kdgK* (SSO3195) gene disruption was generated in *S. solfataricus* PBL2025 as described previously [24,25]. For construction of the plasmid pSVA3195KO first the upstream flanking region was amplified (primers: Up\_for\_3195, 5'-CCCCGGTACCCGTCAAGGGAACC TGGAAGAAT-3'; Up\_rev\_3195, 5'-GGGGCCATGGC CAAA-GCTATTACATCAACCATGATAG-3') and cloned into pET2268 via *KpnI* and *NeoI*. Then the downstream flanking region was amplified (primers: Down\_for\_3195, 5'-CCCCGGATCCCTTGAGGATGCCGAAA-GA-3'; Down\_rev\_3195, 5'-ATGATTGCGGCCGCTTCA-CTGAATCAC

ATCTTTGACC-3') and cloned into pET2268 already containing the upstream flanking region via *Bam*HI and *Not*I. Then 300 ng of plasmid was transformed in competent *S. solfataricus* PBL2025 via electroporation (GenePulser MXcell™; Bio-Rad), recovered in 1 mL water for 10 min at 75 °C and transferred to 50 mL pre-warmed Brock medium [32] supplemented with 0.4% (w/v) lactose. After 13 days 4 mL of the culture were used to inoculate 50 mL of fresh lactose minimal medium. The mutant PBL2025Δ3195 was detected after X-gal screening on Gelrite plates and confirmed by PCR and sequencing with the primers 1557 (5'-AAGCCTGGACTAGGTGTTTC-3') and 1558 (5'-GTGGTTAACGGATCTCTAGGG-3') (Fig. S2). The growth curves of the reference strain PBL2025 and the deletion mutant PBL2025Δ3195 were measured in Brock minimal medium supplemented with 0.2% (w/v) of NZ-Amine, glucose or galactose. For the growth studies 50 mL of pre-warmed medium in long-neck Erlenmeyer flasks was inoculated with pre-cultures (start value  $D_{600\text{ nm}}$  0.005) and incubated at 76 °C and 180 r.p.m., and growth was monitored at  $D_{600\text{ nm}}$ .

#### qRT-PCR analysis of PBL2025Δ3195

Total RNA was isolated from 12 mL early exponential growing cultures ( $D$  0.4) adapted to minimal medium supplemented with 0.4% glucose with Quick-RNA MiniPrep Kit (Zymo Research, Irvine, CA, USA) according to the manufacturer's protocol for cells in suspension. Residual genomic DNA was removed by RNase-free DNaseI treatment (Fermentas, St. Leon Rot, Germany) for 2 h at 37 °C. Successful DNA removal was verified by normal PCR using SSO0685 specific primer pair. Prepared RNA was used for cDNA synthesis using the First Strand cDNA Synthesis Kit (Fermentas) with random hexameric primers following the manufacturer's instructions. Quantitative real-time PCR analysis was performed with the SYBR green detection system of the Real-Time 7300 PCR machine (Applied Biosystems, Darmstadt, Germany) using the Maxima SYBR Green/ROX qPCR Master Mix (Fermentas). Real-Time 7300 PCR software automatically determined the  $C_t$  values after 40 cycles. Gene specific primer sets were used to detect the transcript levels of SSO3194, SSO3197 and the house-keeping gene *Sso0685* (*secY*) as reference in two biological replicas (each in technical replica) of PBL2025 and PBL2025Δ3195. For each primer pair the efficiency was calculated from the linear regression curve of  $C_t$  values of a 10-fold dilution series (1 pg to 1 ng) of *S. solfataricus* genomic DNA as template DNA. The  $C_t$  values of SSO3194 and SSO3197 were standardized to the  $C_t$  values of SSO0685 (*secY*) for each biological replica. Control reactions were performed with DNase I treated RNA as template. For the calculation of transcription fold change transcription levels of parental strain PBL2025 were compared with the transcription levels of deletion mutant PBL2025Δ3195.

#### Metabolome analysis

Cell mass was obtained from cultivation in long-neck flasks at 80 °C, pH 3.5, and 4 g·L<sup>-1</sup> glucose as sole carbon source. *S. solfataricus* PBL2025 and PBL2025ΔSSO3195 grew around 72 h before they reached an  $D_{600}$  of 0.9 at the end of the exponential growth phase. Cells were harvested by centrifugation (3904 g, 5 min, 20 °C). After harvesting, the cell pellet was resuspended (by shaking) in 20 mL 0.9% (w/v) NaCl at room temperature and washed twice (3904 g, 3 min, 20 °C). Subsequently, cells were resuspended in 1.5 mL methanol (containing 60 μL ribitol ( $c = 0.2\text{ g}\cdot\text{L}^{-1}$ ) and lyzed in an ultrasonic bath for 15 min at 70 °C. Afterwards, the sample was incubated on ice for 2 min and 1.5 mL of deionized water was added and vortexed. For extraction of metabolites 1 mL chloroform was added and mixed by vortexing. After centrifugation (3904 g, 5 min, 4 °C) the upper, polar phase was transferred into a fresh tube (2 mL) and dried in a vacuum concentrator (SpeedVac, Eppendorf) for 1 h with rotation and overnight without rotation. The final step was the derivatization of the metabolites for subsequent GC-MS analysis. For this, 20 μL pyridine containing 20 mg·mL<sup>-1</sup> methoxyamine hydrochloride was added to the dried sample (vortex for 1 min). After incubation in a thermomixer (600 r.p.m., 90 min, 30 °C; Thermomixer Comfort, Eppendorf) 32 μL *N*-methyl-*N*-trimethylsilyltrifluoroacetamide was added (vortex for 1 min). Samples were incubated again for 30 min at 37 °C (shaking speed 600 r.p.m.) followed by 120 min at 25 °C (shaking speed 600 r.p.m.). After subsequent centrifugation (10 000 g, 5 min, room temperature) 50 μL of the sample was transferred into a glass vial containing a micro cartridge for GC-MS analysis. GC-MS analysis was performed as described previously [26]. All chromatograms were processed using METABOLITEDETECTOR for untargeted analysis [33].

#### Acknowledgements

This work was supported in the course of the transnational SYSMO (SulfoSYS, P-N-01-09-23) project. BS (0315004A), DS (0315004B), S-VA (0315004C) and PR (183085/S10) thank the Federal Ministry of Education and Research (BMBF), Germany, the Netherlands Organization for Scientific Research (NWO) and the Research Council of Norway (RCN) for financial support.

#### References

- 1 Woese CR & Fox GE (1977) Phylogenetic structure of the prokaryotic domain: the primary kingdoms. *Proc Natl Acad Sci USA* **74**, 5088–5090.
- 2 Verhees CH, Kengen SWM, Tuininga JE, Schut GJ, Adams MWW, De Vos WM & Van Der Oost J (2004) Erratum: The unique features of glycolytic pathways in

- Archaea (*Biochemical Journal* (2003) **375** (231–246)). *Biochem J* **377**, 819–822.
- 3 Siebers B & Schönheit P (2005) Unusual pathways and enzymes of central carbohydrate metabolism in Archaea. *Curr Opin Microbiol* **8**, 695–705.
  - 4 Sato T & Atomi H (2011) Novel metabolic pathways in Archaea. *Curr Opin Microbiol* **14**, 307–314.
  - 5 Zillig W, Stetter KO & Wunderl S (1980) The *Sulfolobus*-‘Caldariella’ group: taxonomy on the basis of the structure of DNA-dependent RNA polymerases. *Arch Microbiol* **125**, 259–269.
  - 6 De Rosa M, Gambacorta A, Nicolaus B, Giardina P, Poerio E & Buonocore V (1984) Glucose metabolism in the extreme thermoacidophilic archaeobacterium *Sulfolobus solfataricus*. *Biochem J* **224**, 407–414.
  - 7 Lamble HJ, Heyer NI, Bull SD, Hough DW & Danson MJ (2003) Metabolic pathway promiscuity in the Archaeon *Sulfolobus solfataricus* revealed by studies on glucose dehydrogenase and 2-keto-3-deoxygluconate aldolase. *J Biol Chem* **278**, 34066–34072.
  - 8 Ahmed H, Ettema TJG, Tjaden B, Geerling ACM, Van Der Oost J & Siebers B (2005) The semi-phosphorylative Entner–Doudoroff pathway in hyperthermophilic archaea: a re-evaluation. *Biochem J* **390**, 529–540.
  - 9 Haferkamp P, Kutschki S, Treichel J, Hemedá H, Sewczyk K, Hoffmann D, Zaparty M & Siebers B (2011) An additional glucose dehydrogenase from *Sulfolobus solfataricus*: fine-tuning of sugar degradation? *Biochem Soc Trans* **39**, 77–81.
  - 10 Lamble HJ, Milburn CC, Taylor GL, Hough DW & Danson MJ (2004) Gluconate dehydratase from the promiscuous Entner–Doudoroff pathway in *Sulfolobus solfataricus*. *FEBS Lett* **576**, 133–136.
  - 11 Kim S & Lee SB (2005) Identification and characterization of *Sulfolobus solfataricus* D-gluconate dehydratase: a key enzyme in the non-phosphorylated Entner–Doudoroff pathway. *Biochem J* **387**, 271–280.
  - 12 Lamble HJ, Theodossis A, Milburn CC, Taylor GL, Bull SD, Hough DW & Danson MJ (2005) Promiscuity in the part-phosphorylative Entner–Doudoroff pathway of the archaeon *Sulfolobus solfataricus*. *FEBS Lett* **579**, 6865–6869.
  - 13 Ettema TJG, Ahmed H, Geerling ACM, Van Der Oost J & Siebers B (2008) The non-phosphorylating glyceraldehyde-3-phosphate dehydrogenase (GAPN) of *Sulfolobus solfataricus*: a key-enzyme of the semi-phosphorylative branch of the Entner–Doudoroff pathway. *Extremophiles* **12**, 75–88.
  - 14 Potters MB, Solow BT, Bischoff KM, Graham DE, Lower BH, Helm R & Kennelly PJ (2003) Phosphoprotein with phosphoglycerate mutase activity from the archaeon *Sulfolobus solfataricus*. *J Bacteriol* **185**, 2112–2121.
  - 15 Kardinahl S, Schmidt CL, Hansen T, Anemüller S, Petersen A & Schäfer G (1999) The strict molybdate-dependence of glucose-degradation by the thermoacidophile *Sulfolobus acidocaldarius* reveals the first crenarchaeotic molybdenum containing enzyme – an aldehyde oxidoreductase. *Eur J Biochem* **260**, 540–548.
  - 16 Kehrer D, Ahmed H, Brinkmann H & Siebers B (2007) Glycerate kinase of the hyperthermophilic archaeon *Thermoproteus tenax*: new insights into the phylogenetic distribution and physiological role of members of the three different glycerate kinase classes. *BMC Genomics* **8**, 301.
  - 17 Reher M, Bott M & Schönheit P (2006) Characterization of glycerate kinase (2-phosphoglycerate forming), a key enzyme of the nonphosphorylative Entner–Doudoroff pathway, from the thermoacidophilic euryarchaeon *Picrophilus torridus*. *FEMS Microbiol Lett* **259**, 113–119.
  - 18 Noh M, Jung JH & Lee SB (2006) Purification and characterization of glycerate kinase from the thermoacidophilic archaeon *Thermoplasma acidophilum*: an enzyme belonging to the second glycerate kinase family. *Biotechnol Bioprocess Engineer* **11**, 344–350.
  - 19 Liu B, Hong Y, Wu L, Li Z, Ni J, Sheng D & Shen Y (2007) A unique highly thermostable 2-phosphoglycerate forming glycerate kinase from the hyperthermophilic archaeon *Pyrococcus horikoshii*: gene cloning, expression and characterization. *Extremophiles* **11**, 733–739.
  - 20 Liu B, Wu L, Liu T, Hong Y, Shen Y & Ni J (2009) A MOFRL family glycerate kinase from the thermophilic crenarchaeon, *Sulfolobus tokodaii*, with unique enzymatic properties. *Biotechnol Lett* **31**, 1937–1941.
  - 21 Yang C, Rodionov DA, Rodionova IA, Li X & Osterman AL (2008) Glycerate 2-kinase of *Thermotoga maritima* and genomic reconstruction of related metabolic pathways. *J Bacteriol* **190**, 1773–1782.
  - 22 Potter JA, Kerou M, Lamble HJ, Bull SD, Hough DW, Danson MJ & Taylor GL (2008) The structure of *Sulfolobus solfataricus* 2-keto-3-deoxygluconate kinase. *Acta Crystallogr Biol Crystallogr* **64**, 1283–1287.
  - 23 Wagner M, Berkner S, Ajon M, Driessen AJM, Lipps G & Albers SV (2009) Expanding and understanding the genetic toolbox of the hyperthermophilic genus *Sulfolobus*. *Biochem Soc Trans* **37**, 97–101.
  - 24 Albers SV & Driessen AJM (2008) Conditions for gene disruption by homologous recombination of exogenous DNA into the *Sulfolobus solfataricus* genome. *Archaea* **2**, 145–149.
  - 25 Schelert J, Dixit V, Hoang V, Simbahan J, Drozda M & Blum P (2004) Occurrence and characterization of mercury resistance in the hyperthermophilic Archaeon *Sulfolobus solfataricus* by use of gene disruption. *J Bacteriol* **186**, 427–437.

- 26 Zaparty M, Esser D, Gertig S, Haferkamp P, Kouril T, Manica A, Pham TK, Reimann J, Schreiber K, Sierocinski P *et al.* (2009) ‘Hot standards’ for the thermoacidophilic archaeon *Sulfolobus solfataricus*. *Extremophiles* **14**, 119–142.
- 27 Nishimasu H, Fushinobu S, Shoun H & Wakagi T (2006) Identification and characterization of an ATP-dependent hexokinase with broad substrate specificity from the hyperthermophilic archaeon *Sulfolobus tokodaii*. *J Bacteriol* **188**, 2014–2019.
- 28 Nishimasu H, Fushinobu S, Shoun H & Wakagi T (2007) Crystal structures of an ATP-dependent hexokinase with broad substrate specificity from the hyperthermophilic archaeon *Sulfolobus tokodaii*. *J Biol Chem* **282**, 9923–9931.
- 29 Ahmed H, Tjaden B, Hensel R & Siebers B (2004) Embden–Meyerhof–Parnas and Entner–Doudoroff pathways in *Thermoproteus tenax*: metabolic parallelism or specific adaptation? *Biochem Soc Trans* **32**, 303–304.
- 30 Schwarzenbacher R, McMullan D, Krishna SS, Xu Q, Miller MD, Canaves JM, Elsliger MA, Floyd R, Grzechnik SK, Jaroszewski L *et al.* (2006) Crystal structure of a glycerate kinase (TM1585) from *Thermotoga maritima* at 2.70 Å resolution reveals a new fold. *Proteins Struct Funct Genet* **65**, 243–248.
- 31 Albers SV, Szabo Z & Driessen AJM (2003) Archaeal homolog of bacterial type IV prepilin signal peptidases with broad substrate specificity. *J Bacteriol* **185**, 3918–3925.
- 32 Brock TD, Brock KM, Belly RT & Weiss RL (1972) *Sulfolobus*: a new genus of sulfur-oxidizing bacteria living at low pH and high temperature. *Archiv Mikrobiol* **84**, 54–68.
- 33 Hiller K, Hangebrauk J, Jäger C, Spura J, Schreiber K & Schomburg D (2009) MetaboliteDetector: comprehensive analysis tool for targeted and nontargeted GC/MS based metabolome analysis. *Anal Chem* **81**, 3429–3439.
- 34 Orita I, Sato T, Yurimoto H, Kato N, Atomi H, Imanaka T & Sakai Y (2006) The Ribulose Monophosphate Pathway Substitutes for the Missing Pentose Phosphate Pathway in the Archaeon *Thermococcus kodakaraensis*. *J Bacteriol* **188**, 4698–4704.
- 35 Zaparty M & Siebers B (2010) Physiology, Metabolism and Enzymology of Thermoacidophiles. In *Extremophiles Handbook* (Horikoshi K, Antranikian G, Bull AT, Robb FT & Stetter KO, eds), pp. 602–639. Springer, Tokyo.

### Supporting information

Additional supporting information may be found in the online version of this article at the publisher’s web site:

**Fig. S1.** Reaction scheme for the possible catalytic mechanism at 80 °C for GK at constant glycerate concentration.

**Fig. S2.** Verification of successful construction of the PBL2025Δ3195 mutant.

**Fig. S3.** qRT-PCR analysis of PBL2025Δ3195.

**Doc. S1.** Derivation of GK activity at constant ATP concentration.